REGULAR ARTICLE

blood advances

Immunophenotypic predictors of influenza vaccine immunogenicity in pediatric hematopoietic cell transplant recipients

Justin Z. Amarin,[1,2] Daniel E. Dulek,[1] Joshua Simmons,[3] Haya Hayek,[1] James D. Chappell,[1] Cindy Hager Nochowicz,[3] Carrie L. Kitko,[1] Jennifer E. Schuster,[4] Flor M. Muñoz,[5,6] Claire E. Bocchini,[5] Elizabeth A. Moulton,[5] Susan E. Coffin,[7] Jason L. Freedman,[7] Monica I. Ardura,[8,9] Rachel L. Wattier,[10] Gabriela Maron,[11] Michael Grimley,[12] Grant Paulsen,[12] Lara Danziger-Isakov,[12] Paul A. Carpenter,[13] Janet A. Englund,[13] Natasha B. Halasa,[1,*] Andrew J. Spieker,[14,*] and Spyros A. Kalams,[3,15,*] for the Pediatric HCT Flu Study Group

[1]Department of Pediatrics, Vanderbilt University Medical Center, Nashville, TN; [2]Epidemiology Doctoral Program, School of Medicine, Vanderbilt University, Nashville, TN; [3]Department of Medicine, Vanderbilt University Medical Center, Nashville, TN; [4]Department of Pediatrics, Children's Mercy Kansas City, Kansas City, MO; [5]Division of Infectious Diseases, Department of Pediatrics and [6]Department of Molecular Virology and Microbiology, Baylor College of Medicine and Texas Children's Hospital, Houston, TX; [7]Department of Pediatrics, Perelman School of Medicine, University of Pennsylvania, Philadelphia, PA; [8]Division of Infectious Diseases and Host Defense Program, Nationwide Children's Hospital, Columbus, OH; [9]Department of Pediatrics, The Ohio State University, Columbus, OH; [10]Department of Pediatrics, University of California San Francisco and Benioff Children's Hospital, San Francisco, CA; [11]Department of Infectious Diseases, St. Jude Children's Research Hospital, Memphis, TN; [12]Department of Pediatrics, University of Cincinnati College of Medicine, Cincinnati Children's Hospital Medical Center, Cincinnati, OH; [13]Department of Pediatrics, University of Washington and Seattle Children's Research Institute, Seattle, WA; [14]Department of Biostatistics, Vanderbilt University Medical Center, Nashville, TN; and [15]Department of Pathology, Microbiology and Immunology, Vanderbilt University, Nashville, TN

Key Points

- Baseline numbers of certain immune cells predicted influenza vaccine immunogenicity in pediatric HCT recipients.
- Immune reconstitution profiles could inform optimal influenza vaccination timing after pediatric HCT.

Pediatric hematopoietic cell transplant (HCT) recipients exhibit poor serologic responses to influenza vaccination early after transplant. To facilitate the optimization of influenza vaccination timing, we sought to identify B- and T-cell subpopulations associated with influenza vaccine immunogenicity in this population. We used mass cytometry to phenotype peripheral blood mononuclear cells collected from pediatric HCT recipients enrolled in a multicenter influenza vaccine trial comparing high- and standard-dose formulations over 3 influenza seasons (2016-2019). We fit linear regression models to estimate relationships between immune cell subpopulation numbers before vaccination and prevaccination to postvaccination geometric mean fold rises in antigen-specific (A/H3N2, A/H1N1, and B/Victoria) serum hemagglutination inhibition antibody titers (28-42 days, and ~6 months after 2 doses). For cell subpopulations identified as predictive of a response to all 3 antigens, we conducted a sensitivity analysis including time after transplant as an additional covariate. Among 156 HCT recipients, we identified 33 distinct immune cell subpopulations; 7 significantly predicted responses to all 3 antigens 28 to 42 days after a 2-dose vaccine series, irrespective of vaccine dose. We also found evidence that baseline absolute numbers of naïve B cells, naïve $CD4^+$ T cells, and circulating T follicular helper cells predicted peak and sustained vaccine-induced titers irrespective of dose or timing of posttransplant vaccine administration. In conclusion, several B- and T-cell subpopulations predicted influenza vaccine immunogenicity in pediatric HCT recipients. This study provides insights into the immune determinants of vaccine responses and may help guide the development of tailored vaccination strategies for this vulnerable population.

Submitted 6 November 2023; accepted 29 January 2024; prepublished online on *Blood Advances* First Edition 22 February 2024; final version published online 10 April 2024. https://doi.org/10.1182/bloodadvances.2023012118.

*N.B.H., A.J.S., and S.A.K. are joint senior authors.

Data are available on request from the corresponding author, Spyros A. Kalams (s.kalams@vumc.org).

The full-text version of this article contains a data supplement.

Introduction

Influenza infection causes significant morbidity among immunocompromised individuals, including pediatric hematopoietic cell transplant (HCT) recipients.[1-4] Pediatric HCT recipients exhibit a suboptimal response to influenza vaccination compared with their immunocompetent counterparts.[5-8] One approach to improve response is to administer high-dose inactivated influenza vaccines.[9-14] In our recent multicenter, randomized controlled trial, a 2-dose series of high-dose trivalent influenza vaccine (HD-TIV) was associated with significantly higher geometric mean hemagglutinin inhibition (HAI) titers against influenza A/H3N2 and A/H1N1 compared with 2 doses of standard-dose quadrivalent influenza vaccine (SD-QIV) in pediatric HCT recipients, 3 to 35 months after transplant.[13,14]

Previous studies of influenza vaccine responses in HCT recipients have identified several factors associated with immunogenicity, including absolute lymphocyte number,[6,15,16] B-cell number,[1,9,17] posttransplant timing of vaccination,[1,14,16-20] concurrent immunosuppressive therapies,[15,18] and graft-versus-host disease.[16,19] Few studies, mainly in adult HCT recipients, have attempted to identify specific immune cell subsets that correlate with vaccine response. The collective findings of these studies identified various B-cell subpopulations as critical to vaccine responses, whereas associations between T-cell subpopulations and immunogenicity were inconsistent.[1,17]

Predictors of influenza vaccine response have not been consistent across studies, possibly because of limitations such as small sample sizes, lack of detailed immunophenotyping, or insufficient representation of HCT recipients in the early posttransplant stage.[1,17] Notably, previous studies that focused specifically on pediatric HCT recipients were underpowered and did not include immunophenotyping.[6] Current guidelines recommend that HCT recipients receive 1 to 2 standard-dose influenza vaccines at least 3 to 6 months after transplant but do not incorporate immunologic parameters to guide vaccination strategies.[21,22]

To address this gap, we sought to identify the association between immune cell subsets, quantified at the time of vaccination, and influenza vaccine immunogenicity using 33-parameter mass cytometry by time of flight (CyTOF) for detailed T- and B-cell phenotyping. Our goal was to identify specific cell subpopulations able to predict vaccine responses in this unique patient population. The identification of these immunologic predictors could inform the optimal timing of influenza vaccination after HCT and facilitate further mechanistic studies on influenza vaccination in individuals who are immunocompromised.

Methods

Study design and participants

The samples for this study were isolated from pediatric HCT recipients who were aged 3 to 17 years, and 3 to 35 months after allogeneic HCT at the time of enrollment in a phase 2, multicenter, double-blinded, randomized controlled trial (www.clinicaltrials.gov identifier: NCT02860039) comparing 2 doses of HD-TIV with 2 doses of SD-QIV at 9 US study sites over 3 consecutive influenza seasons (2016-2017, 2017-2018, and 2018-2019).[13,14] Each study participant was randomized to receive 2, 0.5 mL intramuscular doses of either HD-TIV or SD-QIV with a target interval of 28 to 42 days between vaccine doses (at the time of this study, the HD formulation of the quadrivalent vaccine was not available). Blood collection for serum and peripheral blood mononuclear cells (PBMCs) was performed on the day of the first vaccination, 28 to 42 days after the second vaccination (to estimate peak immunogenicity), and ~6 months after the second vaccination (to estimate sustained immunogenicity). The parent study enrolled 170 participants, all of whom received at least 1 study vaccine. We collected race and ethnicity data from parents or legal guardians to comply with the National Institutes of Health policy and guidelines on the inclusion of women and minorities as subjects in clinical research.

The study was reviewed and approved by the institutional review board at each of the study sites. All parents or guardians provided written informed consent, and participants aged ≥7 years provided assent. Study data were collected and managed using a REDCap database hosted by Vanderbilt University.

Isolation of PBMCs

Overall, PBMCs were isolated from blood samples of 156 pediatric HCT recipients drawn just before the first vaccination; the remaining 14 were excluded from analysis because of low cell viability (n = 10) or lack of a baseline specimen (n = 4). Whole blood was collected into prefilled Leucosep tubes (Greiner Bio-One, Monroe, NC) containing Ficoll-Paque PLUS (GE Health-Care, Piscataway, NJ) and processed on the day of collection. Whole blood was centrifuged at 800*g* for 15 minutes. The buffy coat was removed, pelleted by low-speed centrifugation (400*g*), washed 2 times with phosphate-buffered saline (PBS), and counted on a Coulter Ac·T diff Hematology Analyzer (Beckman Coulter, Brea, CA). The cells were washed a third time and resuspended in media composed of 90% fetal bovine serum (Atlanta Biologicals, Norcross, GA) containing 10% dimethyl sulfoxide (Sigma-Aldrich, St. Louis, MO). Cells were cryopreserved at −80°C in a StrataCooler (Fisher Scientific, Hampton, NH) overnight and transferred to liquid nitrogen storage.

Hemagglutination inhibition assays

Sera were prepared from whole blood and frozen at each site, shipped to Vanderbilt University Medical Center, and then bulk-shipped to Sanofi Global Clinical Immunology for blinded HAI assay testing for each vaccine-specific antigen.[13,14]

Mass cytometry

For each sample, 2×10^6 PBMCs were incubated first with a viability reagent (10 μM cisplatin, Enzo Life Sciences, Farmingdale, NY) in 1 mL serum-free RPMI 1640 for 3 minutes.[23] Cisplatin was quenched by washing once with RPMI 1640 containing 10% fetal bovine serum followed by 2 washes in PBS/1% bovine serum albumin (BSA). A master mix containing 31 antibody-metal conjugates (CyTOF reagents purchased from Fluidigm, Sunnyvale, CA; supplemental Table 1) was added to each sample (100 μL PBS/1% BSA total staining volume) and incubated at room temperature for 30 minutes. Cells were then washed twice with PBS, fixed for 15 minutes with 1.6% paraformaldehyde at room temperature, washed once with PBS, and permeabilized at −20°C in 1 mL 100% cold methanol overnight. The following day, cells were washed at 800*g* with PBS, followed by a PBS/1% BSA wash, and

stained with anti–Ki-67 for 20 minutes at room temperature. Cells were then incubated with 250 nM iridium intercalator (Fluidigm and DVS Sciences, Sunnyvale, CA)[24] in the presence of 1.6% paraformaldehyde for 20 minutes at room temperature before storing at 4°C. Before running on the Helios mass cytometer (CyTOF; Fluidigm), cells were washed twice in PBS, washed once with deionized water, and then resuspended at 5×10^5 cells per mL in deionized water for mass cytometry analysis that day. Before data acquisition, all sample tubes were spiked with EQ Four Element Calibration Beads (Fluidigm). Cells were filtered immediately before injection into the mass cytometer using a 35 μm nylon mesh cell-strainer cap (BD Biosciences, San Jose, CA).

Data acquisition and preliminary analysis

Data were acquired with a Helios CyTOF instrument and CyTOF software version 7.1 for Helios. Dual-count calibration and noise reduction (cell length, 10-75; lower convolution threshold, 10) were applied during acquisition. Data were transformed to "arcsinh" scales with cofactors from 15 to 50.[25]

Mass cytometry gating strategy

Flow cytometry standard files were bead-normalized using the "premessa" R package bead normalization tool and analyzed using FlowJo 10.8.[26,27] $CD45^+$ live singlet cells were identified using a gating strategy proposed by Lee et al.[28]

Batch effects

Data were acquired over the course of 38 runs (batches). A control sample consisting of a biological replicate from a large blood draw from a single individual was included in each run. However, a different PBMC control was used in the last 2 runs because of limited sample availability. To determine whether the inclusion of the last 2 runs was appropriate, a batch effect analysis on the first 36 runs was performed. Initially, bead-normalized $CD45^+$ live singlet events from the 36 technical replicate samples included in the first 36 runs were isolated and concatenated. After applying "arcsinh(x/5)" transform, the "uwot" R package was used to create a uniform manifold approximation and projection (UMAP) from the concatenated files.[29] UMAP mean centers per replicate were charted on the UMAP plot. The mean centers did not show significant variation and no batch-specific UMAP islands or regions were observed. The bead-normalized $CD45^+$ live singlet events were then batch-corrected using the "CytofBatchAdjust" R package.[30] We then performed a formal analysis comparing differences before and after correction. A UMAP was created from concatenated files from uncorrected experimental data and separately on the corrected experimental data. A nearest neighbor search was performed separately on each UMAP plot and the mean batch heterogeneity for each data point's local neighborhood, defined as its 200 nearest neighbors, was quantified. The difference between observed and theoretical heterogeneity was calculated and a paired test showed no significant increase in heterogeneity between the UMAP without correction and the UMAP with correction using this nearest neighbor method ($P = .55$). Given this result, batch correction was not performed, and the last 2 runs were included in the analysis.

Data clustering and visualization

Files with >30 000 $CD45^+$ live singlet events after FlowJo gating were downsampled to 30 000 cells per individual, with a total of 4 321 765 cells for downstream analysis. The downsampled data set was transformed using an "arcsinh(x/5)" transform. After transformation, the "RANN" R package was used to conduct a nearest neighbor search on the data.[31] The "future.apply" R package was used to parallelize the search across 50 threads.[32] A sparse weighted adjacency matrix was then constructed using the "Matrix" R package.[33] Nodes were considered linked to their 30 nearest neighbors (self-exclusive).

The sparse matrix was saved to disk in mtx format and read into Python (version 3.9.12) with the "mmread" method from the "scipy.io" package.[34] The adjacency matrix was passed to the Leiden community detection algorithm using the "leidenalg" package to partition cells into discrete subpopulations.[35] A resolution parameter of 1.5 and seed 123 was used. This produced a total of 33 cell subpopulations. The relative frequencies of these subpopulations were calculated and converted to absolute numbers by multiplying them by each participant's absolute lymphocyte number. The absolute cell subpopulation numbers were used for all downstream statistical tests and reconstitution characterization. To visualize the underlying data structure, the UMAP algorithm was run on the transformed data set using the "umap" Python package with default settings.[36] The "flowCore" R and "FlowKit" Python packages were used to process flow cytometry standard files.[37,38] R (version 4.1) was used to perform pseudorandom operations such as down-sampling.

Statistical analysis

We used R (version 4.3.0) to perform all analyses. Absolute and relative frequencies were used to describe categorical variables and the median and interquartile range (IQR) were used to describe continuous variables. In the regression analyses, we used multiple imputation by chained equations with M = 500 iterations using the "mice" package in R to address missing data. We included 156 individuals in the mass cytometry analysis and cell subpopulation identification as outlined above. However, 2 participants died before postdose 2 titer measurements and were excluded from all regression analyses. Therefore, regression analyses for early postvaccine 2 immunogenicity included data from 154 participants. In addition, 2 participants died after postvaccine 2 measurements but before 6-month measurements; these participants contributed to regression analyses involving postdose 2 titers but were not imputed in analyses of 6-month titers. Therefore, regression analysis for late postvaccine 2 immunogenicity included data from 152 participants. For each combination of antigens featured in both HD-TIV and SD-QIV (ie, A/H3N2, A/H1N1, and B/Victoria) and 33 distinct cell subpopulations, we performed linear regression on log-transformed titers to estimate the relationship between the geometric mean fold-rise (GMFR) in HAI titer, that is, from prevaccination to 28 to 42 days after 2 vaccine doses (or "peak immunogenicity"), and cell number. Cell numbers were modeled using the transformation $\log(x + 1)$ so that an observed cell subpopulation number of 0 was mapped to 0 under the transformation while preserving monotonicity. To improve precision, we included the intervention group (ie, HD-TIV or SD-QIV) as a covariate because it is highly predictive of postvaccine titer. Furthermore, we used the Benjamini-Yekutieli method to adjust P values for multiplicity, thereby controlling the false discovery rate; P values based on this adjustment were declared statistically significant based on a nominal threshold of $\alpha = .05$. For cell

subpopulations identified as predicting response to all 3 antigens, we performed subsequent sensitivity analyses including time after transplant as an additional covariate to determine whether these subpopulations provide additional value in predicting vaccine immunogenicity beyond time after transplant as a proxy for immune reconstitution. Our secondary analysis (and associated sensitivity analysis) involved HAI titers ~6 months after the second dose (or "sustained immunogenicity"), for which our approach mirrored that of the primary analysis. In this sensitivity analysis for sustained immunogenicity, we also included subpopulations that predicted peak immunogenicity against all 3 antigens in the primary analysis.

Results

Clinical characteristics of the cohort

PBMCs were available from blood samples of 156 pediatric HCT recipients drawn immediately before the first vaccination, and these individuals comprised the analytic sample. The median age at first vaccination was 11.8 years (IQR, 6.8-14.3), with a male representation of 56.4% (n = 88 individuals). The race and ethnicity distribution of our cohort, as reported by parents or legal guardians, was as follows: non-Hispanic American Indian or Alaska Native (n = 1; 0.6%), non-Hispanic Asian (n = 6; 3.8%), non-Hispanic Black (n = 27; 17.3%), Hispanic or Latino (n = 33; 21.2%), non-Hispanic White (n = 77; 49.4%), and non-Hispanic other (n = 12; 7.7%). The non-Hispanic other category included non-Hispanic Indian (n = 1; 0.6%), non-Hispanic Indian American (n = 1; 0.6%), non-Hispanic Middle Eastern (n = 2; 1.3%), non-Hispanic multiracial (n = 3; 1.9%), and unknown or unspecified (n = 5; 3.2%). The most common reason for transplantation was malignancy (n = 84; 53.8%), and the median time from transplant to first vaccination was 8.0 months (IQR, 4.6-13.6). A total of 79 individuals (50.6%) were randomized to HD-TIV, and 77 were randomized to SD-QIV (49.4%). The clinical characteristics of the study cohort are detailed in supplemental Table 2.

Identification of immune cell subpopulations

We identified 33 distinct immune cell subpopulations by mass cytometry. Major islands included B cells, $CD4^+$ T cells, and $CD8^+$ T cells (Figure 1). The panel of markers that we used effectively differentiated various T-cell subpopulations, including naïve $CD4^+$ T cells ($CD4^+$ Tn; $CD45RO^-$ $CCR7^+$; subpopulations 5, 7, and 21), naïve $CD8^+$ T cells ($CD8^+$ Tn; subpopulation 8), $CD4^+$ central and effector memory T cells ($CD45RO^+$; subpopulations 2, 12, 19, 20, and 24), and $CD8^+$ central memory T cells and effector memory T cells (subpopulations 6, 9, 15, 16, and 23; Figures 1 and 2).

Associations between baseline cell numbers and peak immunogenicity

The median absolute $CD19^+$, $CD4^+$, and $CD8^+$ numbers at baseline were 384 (IQR, 152-677), 347 (IQR, 189-611), and 325

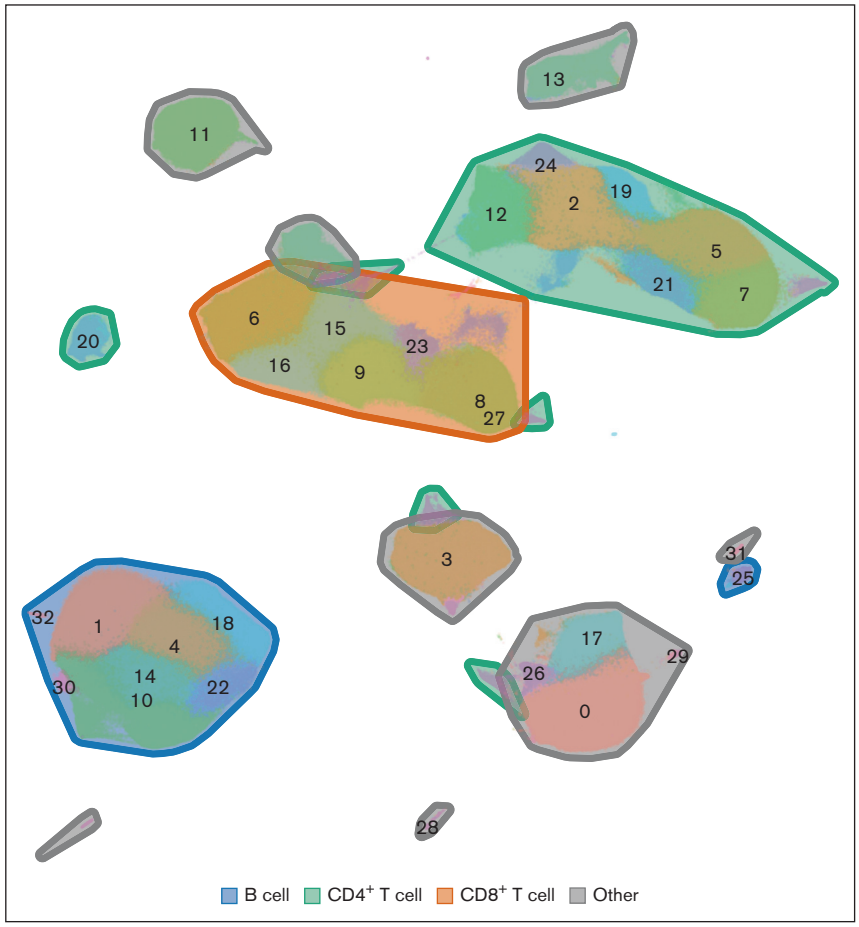

Figure 1. UMAP from a 33-parameter CyTOF antibody panel. This UMAP was generated from 156 pediatric HCT recipients before influenza vaccination. Major islands of B cells, $CD4^+$ T cells, and $CD8^+$ T cells are demarcated.

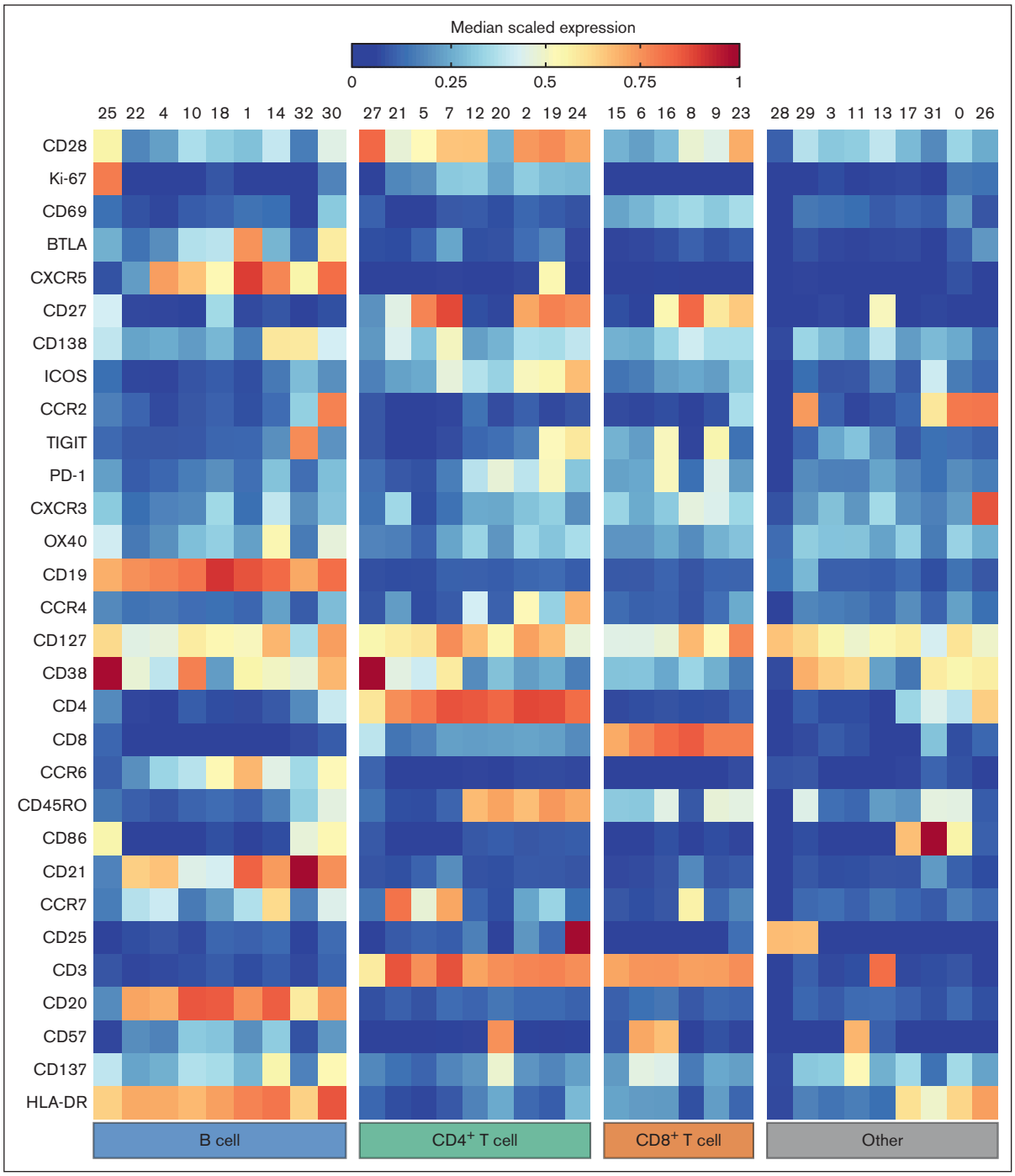

Figure 2. Heat map of cell subpopulations identified by CyTOF. The numbers of several cell subpopulations predicted subsequent serological responses to multiple vaccine immunogens, including 1 and 18 (B cells), 5 and 7 (naïve $CD4^+$ T cells), 19 (cTfh cells), and 23 (memory $CD8^+$ T cells).

cells per μL (IQR, 127-659), respectively. For each antigen, our analyses showed a statistically significant association between higher absolute $CD19^+$ and $CD4^+$ numbers at baseline and increased vaccine immunogenicity at 28 to 42 days after 2 vaccine doses. In contrast, we did not find sufficient evidence of an association between the absolute $CD8^+$ number at baseline and peak vaccine immunogenicity, except for A/H3N2 (supplemental Table 3).

Analysis of B-cell subpopulations showed that 3 of 9 identified subpopulations (1, 4, and 18) were statistically significantly associated with peak vaccine immunogenicity for all 3 antigens (Table 1). These B-cell subpopulations were adjacent to each other on the UMAP (Figure 1), and had similar expression of CXCR5, CD20, and HLA-DR, and either absent (subpopulations 1 and 4) or low (subpopulation 18) CD27 expression, suggesting these were naïve or early memory B-cell subpopulations (Figure 2). Each of

Table 1. Linear regression models estimating the relationship between baseline cell numbers and GMFR of influenza antibody titers from before to 28-42 days after vaccination, adjusted for influenza vaccine dose, in 154 pediatric HCT recipients

	A/H3N2		A/H1N1		B/Victoria	
	Estimate (95% CI)	*P* value	Estimate (95% CI)	*P* value	Estimate (95% CI)	*P* value
B-cell subpopulations						
18*	1.51 (1.32-1.74)	**<.001**	1.40 (1.22-1.61)	**<.001**	1.62 (1.43-1.83)	**<.001**
14	1.25 (1.11-1.41)	**.005**	1.12 (0.99-1.26)	.49	1.22 (1.10-1.36)	**.003**
4*	1.23 (1.10-1.37)	**.008**	1.20 (1.07-1.34)	**.026**	1.31 (1.18-1.46)	**<.001**
1*	1.23 (1.09-1.39)	**.010**	1.23 (1.10-1.37)	**.008**	1.28 (1.15-1.43)	**<.001**
30	1.94 (1.23-3.06)	.057	1.76 (1.14-2.70)	.14	1.82 (1.10-3.01)	.17
10	1.17 (1.03-1.33)	.16	1.13 (1.00-1.28)	.46	1.22 (1.08-1.39)	**.022**
25	1.28 (1.02-1.60)	.28	1.28 (1.04-1.59)	.23	1.44 (1.16-1.79)	**.010**
32	2.86 (0.95-8.65)	.45	3.88 (1.42-10.6)	.12	6.69 (2.70-16.6)	**<.001**
22	1.11 (0.92-1.32)	>.99	1.13 (0.96-1.32)	.97	1.16 (0.97-1.38)	.70
$CD4^+$ T-cell subpopulations						
7*	1.33 (1.18-1.51)	**<.001**	1.25 (1.12-1.41)	**.004**	1.30 (1.16-1.46)	**<.001**
19*	1.40 (1.19-1.65)	**.001**	1.33 (1.13-1.55)	**.009**	1.43 (1.23-1.66)	**<.001**
5*	1.24 (1.09-1.40)	**.012**	1.25 (1.12-1.40)	**.004**	1.26 (1.12-1.41)	**.002**
24	1.54 (1.19-2.01)	**.017**	1.32 (1.04-1.68)	.23	1.40 (1.08-1.80)	.10
2	1.43 (1.10-1.85)	.087	1.33 (1.01-1.74)	.35	1.35 (1.04-1.74)	.19
21	1.24 (1.04-1.49)	.16	1.21 (1.02-1.43)	.28	1.23 (1.04-1.46)	.17
12	1.07 (0.84-1.36)	>.99	1.06 (0.84-1.34)	>.99	1.11 (0.86-1.42)	>.99
20	0.99 (0.85-1.15)	>.99	1.04 (0.89-1.21)	>.99	1.00 (0.85-1.17)	>.99
27	0.84 (0.62-1.14)	>.99	0.93 (0.70-1.24)	>.99	0.95 (0.69-1.30)	>.99
$CD8^+$ T-cell subpopulations						
8*	1.33 (1.17-1.51)	**<.001**	1.29 (1.15-1.46)	**.002**	1.33 (1.18-1.49)	**<.001**
23	1.70 (1.34-2.15)	**<.001**	1.42 (1.12-1.79)	.056	1.69 (1.38-2.08)	**<.001**
16	1.20 (1.00-1.43)	.36	1.12 (0.94-1.33)	>.99	1.11 (0.94-1.30)	>.99
9	1.20 (1.00-1.44)	.39	1.15 (0.95-1.39)	.97	1.14 (0.96-1.35)	.91
15	0.88 (0.75-1.03)	.65	0.94 (0.81-1.09)	>.99	0.93 (0.80-1.08)	>.99
6	0.95 (0.84-1.07)	>.99	0.97 (0.86-1.10)	>.99	0.99 (0.87-1.12)	>.99
Unclassified subpopulations						
13	1.20 (1.00-1.43)	.36	1.17 (0.98-1.39)	.62	1.20 (1.00-1.44)	.34
3	0.80 (0.63-1.01)	.45	0.75 (0.59-0.94)	.15	0.77 (0.59-0.99)	.34
29	1.59 (0.87-2.90)	.81	1.43 (0.81-2.52)	>.99	1.13 (0.70-1.81)	>.99
0	1.00 (0.83-1.21)	>.99	0.94 (0.78-1.14)	>.99	0.98 (0.83-1.16)	>.99
11	1.14 (0.92-1.40)	>.99	1.15 (0.95-1.40)	.97	1.19 (0.97-1.47)	.70
17	0.95 (0.76-1.19)	>.99	1.00 (0.82-1.22)	>.99	0.90 (0.72-1.11)	>.99
26	1.15 (0.91-1.45)	>.99	1.10 (0.88-1.38)	>.99	1.22 (0.96-1.54)	.70
28	0.92 (0.66-1.29)	>.99	0.99 (0.72-1.35)	>.99	0.90 (0.67-1.22)	>.99
31	1.36 (0.61-3.01)	>.99	0.99 (0.51-1.95)	>.99	1.01 (0.55-1.87)	>.99

Log-transformed GMFR from before to after vaccination, 28 to 42 days after 2 doses. Boldface *P* values are statistically significant at a nominal threshold of α=0.05.
CI, confidence interval.
*Statistically significant predictor of GMFR in serum HAI antibody titers for all 3 antigens after 2 vaccine doses.

these cell subpopulations expressed CCR6, with subpopulation 1 having the highest expression. Subpopulation 1 also had the highest level of B and T lymphocyte attenuator expression. The remaining B-cell subpopulations showed variable associations with the peak response to 2 (subpopulation 14), 1 (subpopulations 10, 25, and 32), or none (subpopulations 22 and 30) of the antigens. Similarly, 3 of 9 $CD4^+$ T-cell subpopulations (5, 7, and 19) were associated with higher GMFRs for all 3 antigens. Subpopulations 5 and 7 were related $CD4^+$ Tn cells, each $CD45RO^-$ and expressing CCR7, CD27, CD28, and CD127 to varying degrees. Subpopulation 19 was identified as circulating T follicular helper (cTfh) cells ($CD4^+$ $CXCR5^+$ programmed cell death protein 1^+).

Subpopulation 24 ($CD4^+$ $CD25^+$ $CD127^{low}$ regulatory T cells) was associated with a higher GMFR for A/H3N2 only.

Of the 6 identified $CD8^+$ T-cell subpopulations, only subpopulation 8 ($CD8^+$ Tn cells) showed associations with subsequent peak antibody titers for all 3 antigens. Subpopulation 23 (memory $CD8^+$ T cells) was associated with higher GMFRs for A/H3N2 and B/Victoria, but not A/H1N1. No other subpopulations were found to be associated with the peak vaccine response to any of the antigens (Table 1).

The cell numbers for each of the 7 subpopulations associated with the peak response to all 3 antigens were positively correlated with time after transplant (Figure 3 for A/H3N2; supplemental Figure 1 for A/H1N1; and supplemental Figure 2 for B/Victoria). These figures also depict the fold change in HAI titer from before to after vaccination for each individual. Supplemental Figures 3-5 reproduce the correlations between cell numbers and time after transplant but with individuals stratified using an HAI titer cutoff of 1:110 (<1:110 or ≥1:110; a proxy for seroprotection).[39] We also found that the numbers of these 7 cell subpopulations were positively correlated. For example, the numbers of the 2 $CD4^+$ Tn cell subpopulations (5 and 7) and $CD8^+$ Tn cell subpopulation 8 were the most highly correlated (Spearman $\rho > 0.80$). However, they were less well correlated with the numbers of other important cell subpopulations such as cTfh cells (19) or B-cell subpopulations (4 and 18). This demonstrates that although the number of naïve cells is a measure of the degree of immune reconstitution, it is unlikely that a single subpopulation optimally predicts vaccine response (supplemental Figure 6). Therefore, we performed a sensitivity analysis in which we included time after transplant as an additional covariate. In this analysis, 5 of 7 cell subpopulations were associated with the peak response to at least 2 antigens (all except subpopulations 4 and 5), and among those, B-cell subpopulations 1 and 18, and $CD8^+$ subpopulation 8 (Tn) were associated with the peak response to all 3 antigens (Table 2). $CD4^+$ subpopulations 7 (Tn) and 19 (cTfh) were strongly associated with subsequent A/H3N2 ($P = .005$ and $P = .021$, respectively) and B/Victoria titers ($P = .029$ and $P = .013$, respectively).

Associations between baseline cell numbers and sustained immunogenicity

Having found consistent associations between cell subpopulation numbers and peak HAI titers across our main and sensitivity analyses, we evaluated associations with sustained vaccine immunogenicity (ie, GMFR in HAI titer ~6 months after 2 vaccine doses). We found that B-cell subpopulation 18, which was associated with 28 to 42 day postvaccination immunogenicity, was also associated with sustained vaccine immunogenicity for all 3 antigens, and subpopulation 1 maintained significance for A/H1N1 ($P = .005$) and B/Victoria titers ($P = .002$). The $CD4^+$ Tn (subpopulation 7) and $CD4^+$ cTfh (subpopulation 19) cells maintained their associations with A/H3N2 ($CD4^+$ Tn, $P < .001$; $CD4^+$ cTfh, $P < .001$) and B/Victoria titers ($CD4^+$ Tn, $P < .001$; $CD4^+$ cTfh, $P < .001$). Several other subpopulations identified in the main analysis were associated with sustained vaccine immunogenicity for at least 1 antigen in this analysis (Table 3). A sensitivity analysis that factored in time after transplant showed that B-cell subpopulation 18 remained associated with the sustained response to all 3 antigens, whereas B-cell subpopulation 1 and $CD4^+$ T-cell subpopulations 7 and 19 remained associated with the sustained response to 2 antigens (Table 4). All 4 of these subpopulations (1, 7, 18, and 19) that predicted sustained immunogenicity against at least 2 antigens were also among the 5 subpopulations that predicted peak immunogenicity against at least 2 antigens regardless of influenza vaccine dose and time after transplant.

Discussion

In this study, we leveraged high-dimensional immune profiling to identify candidate predictors of the response to influenza vaccination among 156 pediatric HCT recipients. Analyses in this cohort identified specific B- and T-cell subpopulations associated with the serologic response to vaccination, regardless of vaccine dose. Importantly, several of these associations held even after accounting for the time after transplant, a well-established predictor of immunogenicity. These findings underscore the potential role of specific cellular immune profiles in predicting vaccine immunogenicity and suggest that monitoring profiles such as these could potentially enhance the effectiveness of vaccination strategies in this patient population.

Previous studies have consistently demonstrated a positive relationship between the absolute lymphocyte number, especially the B-cell number, and the HAI antibody response to influenza vaccination in HCT recipients.[1,6,9,15-17] For instance, Karras et al found that higher numbers of unswitched memory B cells and naïve B cells were associated with seroconversion in a cohort of pediatric and adult HCT recipients.[1] Similarly, Roll et al demonstrated that baseline numbers of naïve and memory B cells were associated with the response to pandemic H1N1 (2009) influenza vaccination in adult HCT recipients.[17] Our results corroborate these findings, showing that baseline numbers of several B-cell subpopulations were associated with increased vaccine immunogenicity for ≥1 influenza antigens. We found that circulating absolute numbers of naïve B cells (subpopulation 1; $CD19^+$ $CD20^+$ $CD27^-$) and memory B cells (subpopulation 18; $CD19^+$ $CD20^+$ $CD27^+$)[40] were strongly associated with peak immunogenicity to all 3 vaccine immunogens independent of time after transplant, and the baseline cell numbers of both subpopulations were also associated with sustained serologic responses to all 3 immunogens. This likely explains the association of the absolute B-cell number, an aggregate measure, with antibody responses in previous studies.

In contrast to prior studies, which showed no evidence of an association between overall T-cell numbers and influenza vaccine responses in HCT recipients,[1,17] our detailed CyTOF phenotypic analysis unveiled statistically significant associations between circulating numbers of several specific $CD4^+$ and $CD8^+$ T-cell subpopulations and vaccine immunogenicity. Even with adjustment for time after transplant, the absolute cell numbers of $CD4^+$ Tn cells and memory $CD4^+$ cTfh cells were associated with stronger antibody responses, 28 to 42 days after 2 vaccine doses as well as maintenance of these responses ~6 months after 2 vaccine doses. cTfh cells are known to provide critical help to B cells after antigen exposure. Notably, several studies have shown that the expansion of inducible costimulatory–expressing activated T follicular helper cells during the early postvaccination period is correlated with influenza antibody responses.[41-43] Our study uniquely shows that circulating numbers of cTfh cells have potential predictive value for vaccine responses after HCT.

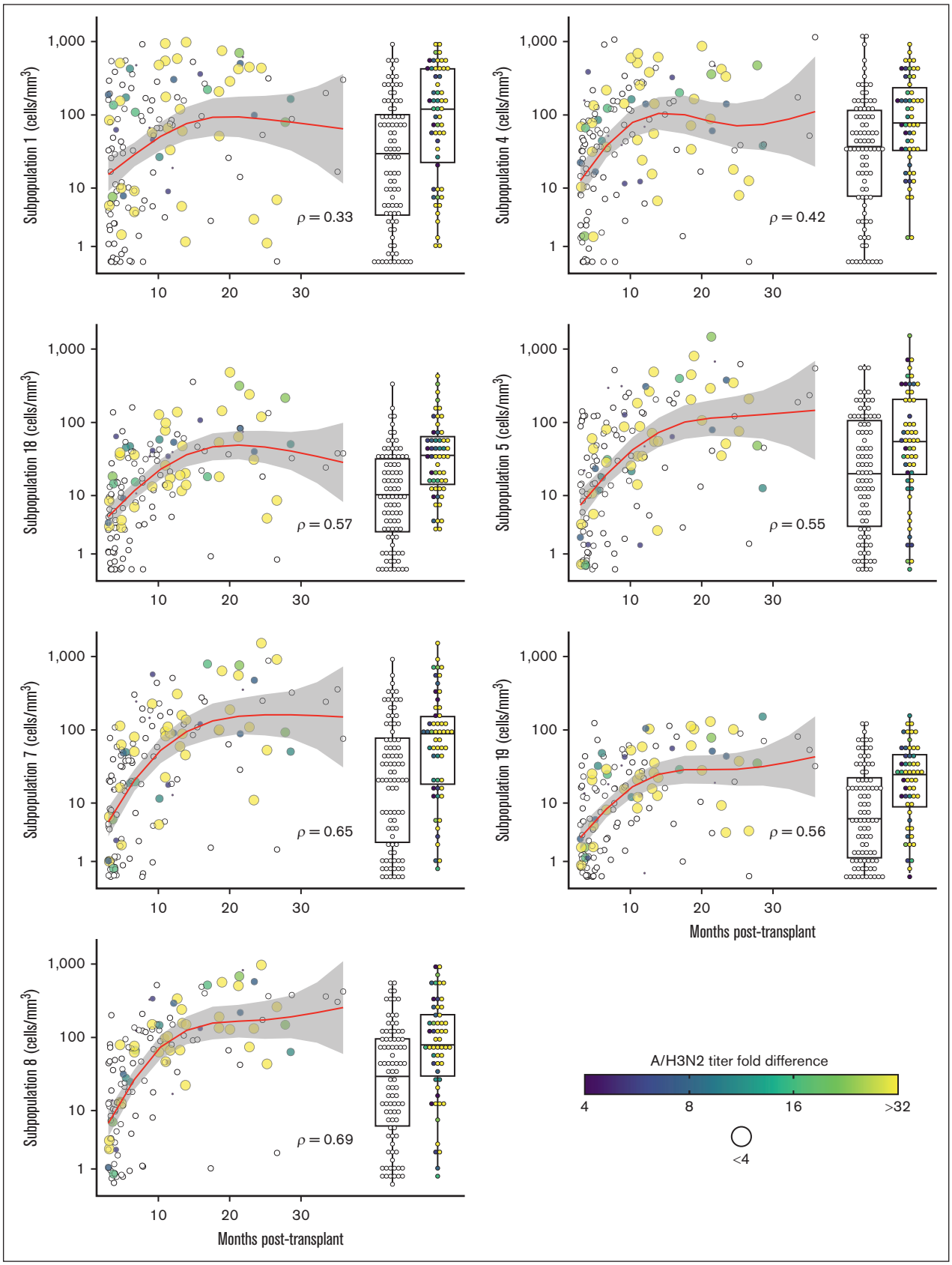

Figure 3.

Table 2. Linear regression models estimating the relationship between baseline cell numbers and GMFR of influenza antibody titers from before to 28-42 days after vaccination, adjusted for influenza vaccine dose and time after transplant, in 154 pediatric HCT recipients

	A/H3N2		A/H1N1		B/Victoria	
	Estimate (95% CI)	*P* value	Estimate (95% CI)	*P* value	Estimate (95% CI)	*P* value
B-cell subpopulations						
18*	1.37 (1.17-1.60)	**<.001**	1.26 (1.08-1.46)	**.003**	1.48 (1.27-1.72)	**<.001**
1*	1.15 (1.03-1.30)	**.016**	1.16 (1.03-1.29)	**.013**	1.20 (1.08-1.34)	**.001**
4	1.13 (0.99-1.28)	.060	1.11 (0.99-1.24)	.085	1.21 (1.08-1.36)	**.001**
$CD4^+$ T-cell subpopulations						
7	1.21 (1.06-1.39)	**.005**	1.13 (0.99-1.29)	.066	1.17 (1.02-1.34)	**.029**
19	1.23 (1.03-1.46)	**.021**	1.16 (0.98-1.37)	.076	1.25 (1.05-1.49)	**.013**
5	1.10 (0.97-1.25)	.15	1.13 (1.00-1.28)	**.049**	1.12 (0.98-1.28)	.10
$CD8^+$ T-cell subpopulations						
8*	1.18 (1.03-1.36)	**.016**	1.16 (1.01-1.33)	**.040**	1.17 (1.02-1.36)	**.030**

Log-transformed GMFR from before to after vaccination, 28 to 42 days after 2 doses. Boldface *P* values are statistically significant at a nominal threshold of α=0.05.
CI, confidence interval.
*Statistically significant predictor of GMFR in serum HAI antibody titers for all 3 antigens after 2 vaccine doses.

We also found that higher baseline numbers of $CD8^+$ Tn cells were associated with stronger antibody responses 28 to 42 days after 2 vaccine doses. Although $CD8^+$ T cells are unlikely to directly influence antibody responses, higher numbers of these cells across time points may reflect differences in the kinetics of immune reconstitution among individuals. The discrepancy between our findings and previous studies is likely explained by the masking of subpopulation-specific effects in aggregated analyses and highlights the importance of examining T-cell subpopulations in more detail.

Our study extends insights from adult HCT recipient cohorts to a pediatric HCT recipient population, indicating that immune profiles in children are associated with influenza vaccination responses, irrespective of vaccine dose and time after transplant. Importantly, the correlations we found between immune cell subpopulations and time after transplant reflect a cross-sectional, rather than longitudinal, analysis; we evaluated all participants at the time of vaccination, albeit at different stages after transplantation. This approach captures the heterogeneity in the rate of immune reconstitution across individuals, which can vary widely and may influence vaccine response. Therefore, although time after transplant is an important surrogate of reconstitution, our findings indicate that enumerating immune cell subpopulations may offer a more precise means of forecasting influenza vaccine immunogenicity and thereby offer potential for individualized influenza vaccination strategies in pediatric HCT recipients. This perspective aligns with previous studies of other vaccines in pediatric HCT recipients, which underscores the potential benefits of an immune recovery–based approach in enhancing vaccine response.[44]

Although sample size may limit the generalizability of our findings, this is, to our knowledge, the largest influenza vaccination study of pediatric HCT recipients to date. Despite this potential limitation, our statistical analyses, which were adjusted for multiplicity, highlighted several consistent associations. Future studies with larger cohorts and different immunocompromised populations, including adult HCT recipients, are warranted to validate our findings. In addition, further research is necessary to determine whether these associations hold for other types of vaccines. Although we did not examine the functional characteristics of the identified cell subpopulations in our study, we predominantly identified naïve cell subpopulations as predictors of vaccine immunogenicity, and it is unlikely that these cells would be antigen reactive. This suggests that individuals with rapid immune reconstitution are more likely to be vaccine responders. The only T-cell memory subpopulation we found to be predictive of immunogenicity were cTfh cells, and numerous studies have confirmed the importance of these cells for the generation of antibody responses.[41,45-50]

Although we used a rather extensive number of antibodies to identify cell subpopulations, it is likely that a more streamlined panel could be useful for assessing individuals in a transplant setting. The addition of antibodies to cell surface markers such as CCR7, CD27, CD28, and CD127 could identify $CD4^+$ and $CD8^+$ Tn cells, CXCR5 and programmed cell death protein 1 could identify cTfh cells, and B and T lymphocyte attenuator and CCR6 could further identify B-cell populations. Our findings also have potential clinical implications, in that with a relatively small number of T- and B-cell markers, individuals at particularly high risk of influenza and its complications but likely to exhibit poor vaccine response, could be identified and targeted for additional or alternative influenza prevention strategies.

In conclusion, our study underscores the value of high-dimensional immune profiling in predicting serologic responses to influenza

Figure 3. Reconstitution of cell subpopulations after pediatric allogeneic HCT. The relationships between time after transplant and each cell subpopulation number per mm^3 of blood are shown (Spearman ρ). The size and color of symbols signify the fold change in HAI titer for A/H3N2 from before to after vaccination (28-42 days after 2 doses). All $P < .001$. Data are presented for 143 individuals. Box plots alongside the main plots are disaggregated by titer fold difference (<4 or ≥4).

Table 3. Linear regression models estimating the relationship between baseline cell numbers and GMFR of influenza antibody titers from before to ~6 months after vaccination, adjusted for influenza vaccine dose, in 152 pediatric HCT recipients

	A/H3N2		A/H1N1		B/Victoria	
	Estimate (95% CI)	*P* value	Estimate (95% CI)	*P* value	Estimate (95% CI)	*P* value
B-cell subpopulations						
18*	1.47 (1.32-1.64)	**<.001**	1.35 (1.16-1.57)	**.012**	1.52 (1.34-1.73)	**<.001**
1	1.21 (1.09-1.34)	**.005**	1.17 (1.04-1.31)	.18	1.22 (1.11-1.35)	**.002**
30	1.88 (1.32-2.66)	**.006**	1.64 (1.09-2.48)	.29	1.66 (1.05-2.61)	.26
4	1.18 (1.07-1.31)	**.016**	1.12 (1.00-1.27)	.64	1.24 (1.11-1.38)	**.002**
25	1.26 (1.05-1.52)	.14	1.25 (1.00-1.55)	.60	1.38 (1.14-1.68)	**.015**
14	1.11 (0.99-1.24)	.59	1.10 (0.97-1.24)	>.99	1.18 (1.05-1.32)	**.049**
10	1.07 (0.94-1.21)	>.99	1.06 (0.92-1.21)	>.99	1.18 (1.03-1.34)	.13
22	1.09 (0.95-1.26)	>.99	1.13 (0.96-1.34)	>.99	1.12 (0.96-1.31)	.81
32	1.39 (0.54-3.53)	>.99	2.08 (0.66-6.54)	>.99	3.21 (1.30-7.91)	.12
CD4$^+$ T-cell subpopulations						
7	1.34 (1.20-1.48)	**<.001**	1.22 (1.08-1.38)	.075	1.28 (1.15-1.43)	**<.001**
5	1.30 (1.17-1.44)	**<.001**	1.19 (1.06-1.34)	.13	1.24 (1.11-1.38)	**.002**
19	1.37 (1.20-1.57)	**<.001**	1.26 (1.06-1.49)	.18	1.43 (1.23-1.66)	**<.001**
24	1.56 (1.26-1.94)	**.001**	1.34 (1.05-1.72)	.29	1.58 (1.22-2.06)	**.008**
21	1.30 (1.12-1.51)	**.006**	1.17 (0.98-1.39)	.89	1.19 (1.02-1.40)	.26
2	1.45 (1.17-1.80)	**.009**	1.27 (0.95-1.69)	.97	1.43 (1.10-1.85)	.075
12	1.08 (0.88-1.33)	>.99	1.10 (0.85-1.42)	>.99	1.23 (0.96-1.57)	.56
20	1.01 (0.88-1.15)	>.99	1.08 (0.92-1.26)	>.99	1.07 (0.93-1.24)	>.99
27	0.96 (0.74-1.24)	>.99	0.90 (0.67-1.21)	>.99	1.09 (0.82-1.46)	>.99
CD8$^+$ T-cell subpopulations						
8	1.33 (1.20-1.49)	**<.001**	1.22 (1.07-1.39)	.098	1.27 (1.14-1.42)	**<.001**
23	1.59 (1.30-1.95)	**<.001**	1.36 (1.08-1.70)	.18	1.63 (1.36-1.96)	**<.001**
15	0.88 (0.77-1.00)	.44	0.92 (0.80-1.06)	>.99	0.93 (0.81-1.07)	>.99
16	1.15 (0.99-1.35)	.50	1.08 (0.90-1.29)	>.99	1.16 (0.99-1.37)	.50
6	0.95 (0.86-1.06)	>.99	0.96 (0.85-1.08)	>.99	1.00 (0.89-1.13)	>.99
9	1.12 (0.95-1.31)	>.99	1.11 (0.92-1.34)	>.99	1.15 (0.99-1.33)	.49
Unclassified subpopulations						
13	1.25 (1.08-1.46)	.037	1.12 (0.92-1.36)	>.99	1.20 (1.01-1.42)	.28
11	1.25 (1.04-1.51)	.17	1.09 (0.88-1.36)	>.99	1.20 (0.99-1.46)	.44
26	1.21 (0.99-1.48)	.46	1.12 (0.89-1.40)	>.99	1.24 (1.00-1.55)	.39
29	1.55 (0.91-2.62)	.70	1.45 (0.85-2.49)	>.99	1.25 (0.80-1.96)	>.99
0	1.12 (0.94-1.34)	>.99	0.98 (0.81-1.19)	>.99	0.98 (0.82-1.16)	>.99
3	0.96 (0.76-1.21)	>.99	0.74 (0.57-0.97)	.38	0.82 (0.65-1.03)	.51
17	1.02 (0.82-1.26)	>.99	1.03 (0.82-1.30)	>.99	0.93 (0.75-1.14)	>.99
28	0.86 (0.65-1.13)	>.99	1.01 (0.75-1.36)	>.99	0.89 (0.65-1.21)	>.99
31	1.08 (0.53-2.20)	>.99	1.13 (0.59-2.20)	>.99	0.92 (0.47-1.81)	>.99

Log-transformed GMFR from before to after vaccination, ~6 months after 2 doses. Boldface *P* values are statistically significant at a nominal threshold of α=0.05.
CI, confidence interval.
*Statistically significant predictor of GMFR in serum HAI antibody titers for all 3 antigens after 2 vaccine doses.

vaccination among pediatric HCT recipients. The cell subpopulations we identified provide crucial insights into the immune determinants of vaccine response, potentially guiding the future development of tailored vaccination strategies or identifying individuals at particularly high risk of poor vaccine response in this vulnerable population. These findings establish a strong foundation for future research focused on optimizing the effectiveness of influenza vaccines specifically in pediatric HCT recipients, and possibly extending to other immunocompromised pediatric and adult populations.

Table 4. Linear regression models estimating the relationship between baseline cell numbers and GMFR of influenza antibody titers from before to ~6 months after vaccination, adjusted for influenza vaccine dose and time after transplant, in 152 pediatric HCT recipients

	A/H3N2		A/H1N1		B/Victoria	
	Estimate (95% CI)	*P* value	Estimate (95% CI)	*P* value	Estimate (95% CI)	*P* value
B-cell subpopulations						
18*	1.34 (1.18-1.51)	**<.001**	1.25 (1.06-1.46)	**.007**	1.40 (1.21-1.62)	**<.001**
1	1.14 (1.03-1.26)	**.011**	1.11 (0.99-1.25)	.079	1.15 (1.04-1.28)	**.007**
4	1.09 (0.98-1.21)	.13	1.05 (0.93-1.19)	.44	1.15 (1.03-1.29)	**.017**
$CD4^+$ T-cell subpopulations						
7	1.24 (1.11-1.40)	**<.001**	1.13 (0.99-1.31)	.079	1.17 (1.03-1.34)	**.016**
5	1.19 (1.07-1.32)	**.001**	1.10 (0.96-1.25)	.17	1.12 (0.99-1.27)	.079
19	1.22 (1.06-1.41)	**.005**	1.13 (0.93-1.38)	.21	1.29 (1.08-1.54)	**.004**
$CD8^+$ T-cell subpopulations						
8	1.22 (1.08-1.38)	**.002**	1.12 (0.96-1.30)	.16	1.14 (0.99-1.31)	.061

Log-transformed GMFR from before to after vaccination, ~6 months after 2 doses. Boldface *P* values are statistically significant at a nominal threshold of α=0.05.
CI, confidence interval.
*Statistically significant predictor of GMFR in serum HAI antibody titers for all 3 antigens after 2 vaccine doses.

Acknowledgments

This work was supported by grants from the National Institute of Allergy and Infectious Diseases (5U01AI125135), the Clinical and Translational Science Awards Program of the National Center for Advancing Translational Sciences (award number UL1TR002243), and the Vanderbilt Infection Pathogenesis and Epidemiology Research T32 (5T32AI007474). Sanofi donated vaccines and performed testing of hemagglutination inhibition. Flow cytometry and data analysis was supported by the Laboratory Sciences Core of the NIH-funded Tennessee Center for AIDS Research (P30 AI110527).

Authorship

Contribution: J.Z.A. contributed to data curation, data analysis, and statistical methodology, and had the primary role of writing, reviewing, and editing the manuscript; D.E.D. provided oversight of the parent trial, and contributed to the writing of the original draft and the review and editing of the manuscript; J.S. was responsible for the organization and interpretation of flow cytometry data, visualized the data, and contributed to the writing of the original draft and the review and editing of the manuscript; H.H. contributed to the review and editing of the manuscript; J.D.C. supervised the acquisition and organization of samples from the parent study and contributed to the review and editing of the manuscript; C.H.N. was primarily responsible for flow cytometry data acquisition, helped organize and interpret data, and contributed to the writing of the original draft and review and editing of the manuscript; C.L.K., J.E.S., C.E.B., E.A.M., F.M.M., S.E.C., J.L.F., M.I.A., R.L.W., G.M., M.G., G.P., L.D.-I., P.A.C., and J.A.E. oversaw study enrollment at the individual sites and contributed to the review and editing of the manuscript; N.B.H. conceptualized, secured funding, provided general oversight of the parent study, oversaw sample collection for subsequent immunology studies, and contributed to the review and editing of the manuscript; A.J.S. oversaw data curation, conceptualized the overall statistical analysis, and contributed to the writing of the original draft and the review and editing of the manuscript; and S.A.K. is the protocol immunologist, oversaw the acquisition and storage of samples from the parent study, conceptualized the immunology study, oversaw data acquisition and analysis, provided data interpretation, and contributed to the writing of the original draft and the review and editing of the manuscript.

Conflict-of-interest disclosure: C.L.K. reports payment for participation on an advisory board for Horizon Therapeutics and Incyte; payment for educational lectures from Medscape, i3 Health, Physicians' Education Resource, and DAVA Oncology; travel support for the Global Summit on Hematologic Malignancies from DAVA Oncology; and payment from CSL Behring for providing graft-versus-host disease adjudication for a clinical trial. J.E.S. reports institutional grants or contracts from the Centers for Disease Control and Prevention, the National Institutes of Health (NIH), and the US Food and Drug Administration; personal consulting fees from the Association of Professionals in Infection Control and Epidemiology and Association of American Medical Colleges; and honoraria for speaking engagements from the Missouri American Academy of Pediatrics. F.M.M. reports grants or contracts (paid to institution) from Gilead for antiviral research, and from Pfizer for vaccine research; grant support from the NIH and the Centers for Disease Control and Prevention; and participation as a data and safety monitoring board member, payments to author from Pfizer and Moderna. C.E.B. reports institutional grants or contracts for clinical trials from Pfizer. E.A.M. reports institutional grants or contracts for clinical trials of pediatric COVID-19 vaccines and therapeutics from Pfizer. S.E.C. reports serving on an advisory board for GlaxoSmithKline (GSK) and receiving research funding from Merck. M.I.A. reports institutional research grants from MiraVista Diagnostics and Merck; consulting fees from Karius; travel support for meeting attendance from the Pediatric Infectious Diseases Society and American Academy of Pediatrics; and reports an unpaid position on the Pediatric Infectious Diseases Society Board of Directors. G.M. reports research support from Astellas Pharma, Inc and SymBio Pharmaceuticals. G.P. reports institutional grants or contracts for

COVID-19 clinical trials and/or respiratory syncytial virus from Pfizer and Moderna, Inc. L.D.-I. reports contracted clinical research support (paid to institution) from Ansun BioPharma, Astellas, AiCuris, Merck, Pfizer, and Takeda; consults for Takeda and Merck; and serves on an advisory panel for Astellas and GSK. J.A.E. reports grant support from AstraZeneca, Merck, Pfizer, and GSK (all paid to institution), and consultant fees from AbbVie, AstraZeneca, Meissa Vaccines, Moderna, Pfizer, Sanofi, Shionogi, and Ark Biopharma. N.B.H. received grant support from Sanofi and Quidel, and reports a current grant from Merck. A.J.S. and S.A.K. report grant support from the NIH. The remaining authors declare no competing financial interests.

A complete list of the members of the Pediatric HCT Flu Study Group appears in supplemental Appendix.

ORCID profiles: J.Z.A., 0000-0002-4484-1077; H.H., 0000-0003-0087-4392; C.H.N., 0000-0003-0094-4952; F.M.M., 0000-0002-0457-7689; C.E.B., 0000-0001-9577-8162; E.A.M., 0000-0003-1751-1395; S.E.C., 0000-0001-9566-5600; J.L.F., 0000-0003-0752-2701; M.G., 0000-0003-2056-5167; G.P., 0000-0002-8901-6513; L.D.-I., 0000-0002-5691-5221.

Correspondence: Spyros A. Kalams, Vanderbilt University Medical Center, Division of Infectious Diseases, 1161 21st Ave S, Nashville, TN 27232; email: s.kalams@vumc.org.

References

1. Karras NA, Weeres M, Sessions W, et al. A randomized trial of one versus two doses of influenza vaccine after allogeneic transplantation. *Biol Blood Marrow Transplant*. 2013;19(1):109-116.
2. Kumar D, Ferreira VH, Blumberg E, et al. A 5-year prospective multicenter evaluation of influenza infection in transplant recipients. *Clin Infect Dis*. 2018;67(9):1322-1329.
3. Danino D, Stanek JR, Rangarajan H, Ardura MI. Hospitalizations for vaccine-preventable infections among pediatric hematopoietic cell transplantation recipients in the first 5 years after transplantation. *Bone Marrow Transplant*. 2021;56(11):2656-2663.
4. Atalla E, Kalligeros M, Mylona EK, et al. Impact of influenza infection among adult and pediatric populations with hematologic malignancy and hematopoietic stem cell transplant: a systematic review and meta-analysis. *Clin Ther*. 2021;43(5):e66-e85.
5. Dulek DE, de St Maurice A, Halasa NB. Vaccines in pediatric transplant recipients-past, present, and future. *Pediatr Transplant*. 2018;22(7):e13282.
6. Ryan AL, Wadia UD, Jacoby P, et al. Immunogenicity of the inactivated influenza vaccine in children who have undergone allogeneic haematopoietic stem cell transplant. *Bone Marrow Transplant*. 2020;55(4):773-779.
7. Miller PDE, de Silva TI, Leonard H, et al. A comparison of viral microneutralization and haemagglutination inhibition assays as measures of seasonal inactivated influenza vaccine immunogenicity in the first year after reduced intensity conditioning, lymphocyte depleted allogeneic haematopoietic stem cell transplant. *Vaccine*. 2019;37(3):452-457.
8. Kang KR, Kim YJ, Ahn MB, et al. Shorter duration of protection and lower geometric mean titers against A/H3N2 antigen of the quadrivalent influenza vaccine in children post-allogeneic hematopoietic stem cell transplantation. *Bone Marrow Transplant*. 2022;57(10):1620-1622.
9. Halasa NB, Savani BN, Asokan I, et al. Randomized double-blind study of the safety and immunogenicity of standard-dose trivalent inactivated influenza vaccine versus high-dose trivalent inactivated influenza vaccine in adult hematopoietic stem cell transplantation patients. *Biol Blood Marrow Transplant*. 2016;22(3):528-535.
10. McManus M, Frangoul H, McCullers JA, Wang L, O'Shea A, Halasa N. Safety of high dose trivalent inactivated influenza vaccine in pediatric patients with acute lymphoblastic leukemia. *Pediatr Blood Cancer*. 2014;61(5):815-820.
11. GiaQuinta S, Michaels MG, McCullers JA, et al. Randomized, double-blind comparison of standard-dose vs. high-dose trivalent inactivated influenza vaccine in pediatric solid organ transplant patients. *Pediatr Transplant*. 2015;19(2):219-228.
12. Haddadin Z, Krueger K, Thomas LD, Overton ET, Ison M, Halasa N. Alternative strategies of posttransplant influenza vaccination in adult solid organ transplant recipients. *Am J Transplant*. 2021;21(3):938-949.
13. Schuster JE, Hamdan L, Dulek DE, et al. Influenza vaccine in pediatric recipients of hematopoietic-cell transplants. *N Engl J Med*. 2023;388(4):374-376.
14. Schuster JE, Hamdan L, Dulek DE, et al. The durability of antibody responses of two doses of high-dose relative to two doses of standard-dose inactivated influenza vaccine in pediatric hematopoietic cell transplant recipients: a multi-center randomized controlled trial. *Clin Infect Dis*. 2024;78(1):217-226.
15. Linnik J, Syedbasha M, Kaltenbach HM, et al. Association of host factors with antibody response to seasonal influenza vaccination in allogeneic hematopoietic stem cell transplant patients. *J Infect Dis*. 2022;225(8):1482-1493.
16. Dhedin N, Krivine A, Le Corre N, et al. Comparable humoral response after two doses of adjuvanted influenza A/H1N1pdm2009 vaccine or natural infection in allogeneic stem cell transplant recipients. *Vaccine*. 2014;32(5):585-591.
17. Roll D, Ammer J, Holler B, et al. Vaccination against pandemic H1N1 (2009) in patients after allogeneic hematopoietic stem cell transplantation: a retrospective analysis. *Infection*. 2012;40(2):153-161.
18. Natori Y, Humar A, Lipton J, et al. A pilot randomized trial of adjuvanted influenza vaccine in adult allogeneic hematopoietic stem cell transplant recipients. *Bone Marrow Transplant*. 2017;52(7):1016-1021.
19. Mohty B, Bel M, Vukicevic M, et al. Graft-versus-host disease is the major determinant of humoral responses to the AS03-adjuvanted influenza A/09/H1N1 vaccine in allogeneic hematopoietic stem cell transplant recipients. *Haematologica*. 2011;96(6):896-904.
20. Issa NC, Marty FM, Gagne LS, et al. Seroprotective titers against 2009 H1N1 influenza A virus after vaccination in allogeneic hematopoietic stem cell transplantation recipients. *Biol Blood Marrow Transplant*. 2011;17(3):434-438.

21. Cordonnier C, Einarsdottir S, Cesaro S, et al. Vaccination of haemopoietic stem cell transplant recipients: guidelines of the 2017 European Conference on Infections in Leukaemia (ECIL 7). *Lancet Infect Dis*. 2019;19(6):e200-e212.
22. Rubin LG, Levin MJ, Ljungman P, et al. 2013 IDSA clinical practice guideline for vaccination of the immunocompromised host. *Clin Infect Dis*. 2014; 58(3):309-318.
23. Nicholas KJ, Greenplate AR, Flaherty DK, et al. Multiparameter analysis of stimulated human peripheral blood mononuclear cells: a comparison of mass and fluorescence cytometry. *Cytometry A*. 2016;89(3):271-280.
24. Ornatsky OI, Lou X, Nitz M, et al. Study of cell antigens and intracellular DNA by identification of element-containing labels and metallointercalators using inductively coupled plasma mass spectrometry. *Anal Chem*. 2008;80(7):2539-2547.
25. Nowicka M, Krieg C, Crowell HL, et al. CyTOF workflow: differential discovery in high-throughput high-dimensional cytometry datasets. *F1000Res*. 2017;6:748.
26. *Premessa*. Parker Institute for Cancer Immunotherapy; 2021. Package release version 0.3.2. Accessed 8 September 2022. https://github.com/ParkerICI/premessa
27. FlowJo Software for Windows. Version 10.8 [Cell Gating]. Accessed 16 July 2021. https://www.flowjo.com/solutions/flowjo/downloads
28. Lee BH, Rahman AH. Acquisition, processing, and quality control of mass cytometry data. *Methods Mol Biol*. 2019;1989:13-31.
29. Melville J. UMAP: Uniform manifold approximation and projection for dimension reduction. Accessed 10 September 2022. https://github.com/jlmelville/uwot
30. Schuyler RP, Jackson C, Garcia-Perez JE, et al. Minimizing batch effects in mass cytometry data. *Front Immunol*. 2019;10:2367.
31. *RANN (R Package, Nearest Neighbor Search)*. Jefferislab; 2019. Package release version 2.6.1. Accessed 12 September 2022. https://github.com/jefferislab/RANN
32. Bengtsson H. A unifying framework for parallel and distributed processing in R using futures. *R J*. 2021;13(2):208-291.
33. Bates D, Maechler M, Jagan M. Matrix: sparse and dense matrix classes and methods. 2022. R Package Version 1.6-4. Accessed 12 September 2022. https://cran.r-project.org/web/packages/Matrix/index.html
34. Virtanen P, Gommers R, Oliphant TE, et al. SciPy 1.0: fundamental algorithms for scientific computing in Python. *Nat Methods*. 2020;17(3):261-272.
35. Traag VA, Waltman L, van Eck NJ. From Louvain to Leiden: guaranteeing well-connected communities. *Sci Rep*. 2019;9(1):5233.
36. Linderman GC, Rachh M, Hoskins JG, Steinerberger S, Kluger Y. Fast interpolation-based t-SNE for improved visualization of single-cell RNA-seq data. *Nat Methods*. 2019;16(3):243-245.
37. Hahne F, LeMeur N, Brinkman RR, et al. flowCore: a bioconductor package for high throughput flow cytometry. *BMC Bioinformatics*. 2009;10:106.
38. White S, Quinn J, Enzor J, et al. FlowKit: a Python toolkit for integrated manual and automated cytometry analysis workflows. *Front Immunol*. 2021;12: 768541.
39. Black S, Nicolay U, Vesikari T, et al. Hemagglutination inhibition antibody titers as a correlate of protection for inactivated influenza vaccines in children. *Pediatr Infect Dis J*. 2011;30(12):1081-1085.
40. Quach TD, Rodriguez-Zhurbenko N, Hopkins TJ, et al. Distinctions among circulating antibody-secreting cell populations, including B-1 cells, in human adult peripheral blood. *J Immunol*. 2016;196(3):1060-1069.
41. Pilkinton MA, Nicholas KJ, Warren CM, et al. Greater activation of peripheral T follicular helper cells following high dose influenza vaccine in older adults forecasts seroconversion. *Vaccine*. 2017;35(2):329-336.
42. Bentebibel SE, Lopez S, Obermoser G, et al. Induction of ICOS+CXCR3+CXCR5+ TH cells correlates with antibody responses to influenza vaccination. *Sci Transl Med*. 2013;5(176):176ra32.
43. Spensieri F, Borgogni E, Zedda L, et al. Human circulating influenza-CD4+ ICOS1+IL-21+ T cells expand after vaccination, exert helper function, and predict antibody responses. *Proc Natl Acad Sci U S A*. 2013;110(35):14330-14335.
44. Carpenter PA, Englund JA. Commentary: is immune recovery-based post-transplantation vaccination in children better than time-based revaccination? *Transplant Cell Ther*. 2021;27(4):281-283.
45. Herati RS, Reuter MA, Dolfi DV, et al. Circulating CXCR5+PD-1+ response predicts influenza vaccine antibody responses in young adults but not elderly adults. *J Immunol*. 2014;193(7):3528-3537.
46. Herati RS, Muselman A, Vella L, et al. Successive annual influenza vaccination induces a recurrent oligoclonotypic memory response in circulating T follicular helper cells. *Sci Immunol*. 2017;2(8):eaag2152.
47. Herati RS, Silva LV, Vella LA, et al. Vaccine-induced ICOS(+)CD38(+) circulating Tfh are sensitive biosensors of age-related changes in inflammatory pathways. *Cell Rep Med*. 2021;2(5):100262.
48. Painter MM, Mathew D, Goel RR, et al. Rapid induction of antigen-specific CD4(+) T cells is associated with coordinated humoral and cellular immunity to SARS-CoV-2 mRNA vaccination. *Immunity*. 2021;54(9):2133-2142.e3.
49. Pallikkuth S, Parmigiani A, Silva SY, et al. Impaired peripheral blood T-follicular helper cell function in HIV-infected nonresponders to the 2009 H1N1/09 vaccine. *Blood*. 2012;120(5):985-993.
50. Pallikkuth S, de Armas L, Rinaldi S, Pahwa S. T follicular helper cells and B cell dysfunction in aging and HIV-1 infection. *Front Immunol*. 2017;8:1380.